ARTICLE

Vanadium aminophenolates in catechol oxidation: conformity with Finke's common catalyst hypothesis

Received 00th January 20xx,
Accepted 00th January 20xx

DOI: 10.1039/x0xx00000x

Pasi Salonen,[a] Risto Savela,[b] Anssi Peuronen,[a] and Ari Lehtonen*[a]

Six known aminophenolate vanadium complexes **V1**–**V6** were examined in 3,5-di-*tert*-butylcatechol (**1**, 3,5-DTBC) oxidation. From the complexes **V1**–**V5** have been previously shown to demonstrate catechol oxidase-like (catecholase) behavior, catalytically oxidizing **1** to 3,5-di-*tert*-butyl-1,2-benzoquinone (**2**, 3,5-DTBQ). A critical re-evaluation of **V1**–**V5**, including **V6** not assessed earlier, in the aerobic oxidation of **1** has revealed that several catechol dioxygenase products are obtained in addition to **2**, which is produced partly by autoxidation. Mechanistic investigations into the **V1**–**V6** catalyzed oxidation of **1** by EPR, negative mode ESI-MS and ^{51}V NMR, in addition to semi-quantitative product distribution analyses with GC and column chromatography afford compelling evidence in support of the "common catalyst hypothesis" earlier proposed by Finke and co-workers. During the reaction, **V1**–**V6** are partially converted *in-situ* by H_2O_2 assisted leaching to vanadium catecholate complexes [V(3,5-DTBC)$_2$(3,5-DTBSQ$^\bullet$)] and [VO(3,5-DTBC)(3,5-DTBSQ$^\bullet$)], where 3,5-DTBSQ$^\bullet$ = 3,5-di-*tert*-butyl-1,2-semiquinone, the latter of which has been implicated as the common true active catalyst in catechol dioxygenation as per the common catalyst hypothesis. The results herein suggest that vanadium aminophenolate complexes are sensitive to H_2O_2 mediated leaching in the presence of strong σ and π donating ligands such as **1** and **2**. Furthermore, based on these results, the use of vanadium aminophenolate complexes as catechol oxidase mimics is not as warranted as previously understood.

Introduction

The use of artificial metal complexes capable of activating dioxygen (O_2) for controlled and mild oxidation of hydrocarbons is regarded as a "Holy grail" technology in oxidation catalysis,[1,2] since O_2 is widely abundant and environmentally compatible. Nature has perfected the use of O_2 as an oxidant in biochemical oxidation reactions catalyzed by metalloenzymes such as catechol oxidase[3,4] and the catechol dioxygenases.[5–7] Catechol oxidase is Cu-dependent enzyme that catalyzes the aerobic oxidation of a variety of catechols to the corresponding benzoquinones, generating water as a by-product. In contrast, Fe-dependent catechol dioxygenases catalyze the oxidative degradation of aromatic compounds by incorporating both oxygen atoms into the end-product(s). The biomimetic functional modeling of catechol oxidase/dioxygenases is of utmost importance to the understanding of the function of the enzymes, their structure and underlying catalytic mechanisms. Consequently, the research into biomimetic models of catechol oxidase/dioxygenases has been very active, and a number of different transition metal complexes have been shown to functionally mimic these enzymes.[8–10]

From the various transition metals, it is well established that vanadium readily reacts with a variety of catechols, forming redox non-innocent complexes.[11–15] Moreover, vanadium has long been recognized to mediate catalytic catechol dioxygenase-like reactions.[16,17] Comparatively recently, however, several groups,[18–22] including ours,[23–25] have engaged in studying the catechol oxidase mimetic properties of various vanadium complexes bearing multidentate aminophenolate class or similar ligands. Having been inspired earlier by the moderate cobalt-catalyzed catecholase activities obtained by others,[26] we recently evaluated a structurally similar vanadium complex **V1** (**Figure 1**) in the oxidation of **1** as a functional model of catechol oxidase.[24] However, it was rapidly realized that **V1** generated a number of products aside from the desired oxidase product **2** (**Table 5**, entry 2). Further investigations into the **V1** catecholase mechanism by means of ^{51}V NMR, negative mode ESI-MS and product selectivity studies pointed towards a "common catalyst hypothesis" which was proposed by Finke and co-workers in 2005 to account for rather similar product selectivities in the oxidation of **1** obtained by structurally diverse V-containing compounds.[27]

According to the seminal work by Finke and co-workers,[27–30] the oxidation of **1** catalyzed by virtually any polyoxometalate-based V-precursor catalyst, and some other simple V-precursors such as [VO(acac)$_2$], regardless of their structure, proceeds *via* the same *autocatalytic* mechanism. This is primarily evidenced by a very similar product distribution comprising of several autoxidation, intra-, and extradiol products **2**–**6** (**Table 5**, entry 1).[27–30] The first, and crucial step in the "autoxidation-product-

[a] Group of Inorganic Materials Chemistry, Department of Chemistry, University of Turku, FI-20014 Turku, Finland.
[b] Laboratory of Molecular Science and Technology, Åbo Akademi University, FI-20500 Turku, Finland.
Electronic Supplementary Information (ESI) available: [details of any supplementary information available should be included here]. See DOI: 10.1039/x0xx00000x

initiated-dioxygenase"[29] mechanism is the non-catalytic autoxidation of **1** by O_2, producing **2** and H_2O_2. In the next step, the generated H_2O_2 then leaches vanadium from the vanadium catalyst precursors, and in the presence of excess **1**, [V(3,5-DTBC)$_2$(3,5-DTBSQ$^\bullet$)] is formed. Subsequently, [V(3,5-DTBC)$_2$(3,5-DTBSQ$^\bullet$)] is oxidized by O_2 to [VO(3,5-DTBC)(3,5-DTBSQ$^\bullet$)]$_2$, also known as Pierpont's complex.[11,29] Pierpont's complex has been implicated to be the catalytic resting state of the true active catalyst, namely the half-fragment [VO(3,5-DTBC)(3,5-DTBSQ$^\bullet$)], which then feeds into new separate catalytic cycles, forming the various catechol oxidation products **3**–**6** according to a general dioxygenase mechanism (ESI Scheme S1).[30] While the crucial active catalyst formation is driven by H_2O_2, via leaching from the vanadium-containing catalyst precursors, the dioxygenase-like reactions require O_2 as the terminal oxidant, and not H_2O_2.

Armed with this knowledge, three key questions regarding the common catalyst hypothesis were tested for **V1**–**V6** and subsequently answered. Firstly, do the product distribution experiments from the **V1**-**V6** catalyzed oxidation of **1** yield a similar if not identical result to that found by Finke and co-workers? Secondly, what is the role of H_2O_2, which is generated *in-situ* during the initial aerobic autoxidation of **1** to **2** with regards to the true catalyst evolution from **V1**–**V6**? Additionally, does H_2O_2 itself confer any effect with respect to the product distribution, *i.e.* can it also act as a terminal oxidant? The third question, intimately connected to the second one: can EPR spectroscopy be used to probe the ultimate fate of **V1**–**V6** during catalysis, and most importantly, can Pierpont's complex be detected in the reaction media?

In this work, we seek to critically re-evaluate **V1**–**V5** (**Figure 1**) as catechol oxidation pre-catalysts. Earlier we have shown by *in-situ* UV-Vis spectroscopy that **1** is aerobically oxidized to **2** in the presence of catalytic amounts of **V1**–**V5**.[31] However, after findings concerning **V1**-catalyzed oxidation of **1**,[24] we deemed a more rigorous re-assessment of **V2**–**V5** sensible. The results and conclusions from the investigations herein offer substantial evidence to suggest that **V1**–**V5** do not display appreciable catechol oxidase-like activity, as previously reported. Rather, under catalytic conditions in the presence of excess **1** the pre-catalysts are converted by H_2O_2 assisted leaching to mixed catecholate/semiquinone bearing non-oxo and oxo vanadium complexes [V(3,5-DTBC)$_2$(3,5-DTBSQ$^\bullet$)] as well as [VO(3,5-DTBC)(3,5-DTBSQ$^\bullet$)], as determined by negative mode ESI-MS spectrometry, EPR and ^{51}V NMR spectroscopy. Moreover, semi-quantitative product distribution analyses by means of column and gas chromatography reveal that a very similar product distribution comprising of the "oxidase" product **2**, as well as several intra- and extradiol dioxygenase products **3**–**5** is obtained with each of the pre-catalysts. These results strongly suggest that all studied V complexes operate via the same common mechanism, as proposed by Finke and co-workers.

Since a crucial step in the common mechanism is the H_2O_2-mediated leaching of vanadium from the pre-catalysts, it was envisioned that **V6**, a complex based on two tetradentate ligands derived from **1**, would be stable towards H_2O_2 and other powerful σ- and π-donor chelating ligands, such as **1**. In this way the perceived stability of **V6** would prevent the *in-situ* formation of Pierpont's complex, thus preventing the formation of the dioxygenase products **3**–**5**. Unfortunately, the structure of **V6** offered no benefits over the other pre-catalysts. Additionally, an extensive set of control reactions revealed that **2** may be obtained under anaerobic conditions using two equivalents of H_2O_2, the reaction progressing both non-catalytically and in the presence of 1 mol-% of the vanadium pre-catalysts.

Experimental section

General

All syntheses, manipulations and experiments were performed under ambient conditions using analytical grade solvents and commercially available reagents, which were used as received without purification or drying procedures, unless mentioned otherwise. All IR spectra were measured using a Bruker VERTEX 70 FTIR instrument equipped with a RT-DLaDTGS detector. 64 scans were performed for each individual measurement using a Harrick VideoMVP™ Single Reflection ATR Microsampler accessory, with a resolution of 4 cm^{-1}. The spectra are measured in transmittance mode, and peaks are reported in wavenumbers (cm^{-1}) and intensities (b = broad, w = weak, m = medium, s = strong, vs = very strong). All NMR spectra were recorded on a Bruker Avance III 400 MHz instrument (^{1}H: 400.00 MHz, ^{13}C: 100.59 MHz) or 500 MHz instrument (^{1}H: 500.08 MHz, ^{13}C: 125.75 MHz, ^{51}V: 131.56 MHz) both equipped with a broad-band smart probes or on a Bruker Avance III 600 MHz instrument (^{1}H: 600.16 MHz, ^{13}C: 150.91 MHz) equipped with a CryoProbe Prodigy triple resonance inverse (TCI) probe, respectively. All ^{1}H and ^{13}C NMR spectra are referenced to residual solvent signals *e.g.* $CHCl_3$-H (^{1}H: δ 7.26, ^{13}C: δ 77.16), DMSO-H6 (^{1}H: δ 2.50, ^{13}C: δ 39.52), acetone-H6 (^{1}H: δ 2.05, ^{13}C: δ 206.26, 29.84), toluene-H8 (^{1}H: 2.08, 6.97, 7.01, 7.09; ^{13}C: δ 137.48, 128.87, 127.96, 125.13, 20.43), regardless if tetramethylsilane (TMS, δ = 0.00 ppm) is present, according to published data.[32] The 0 ppm vanadium reference frequency was calculated from the TMS ^{1}H frequency using the unified chemical shift scale by IUPAC (Ξ(^{51}V, $VOCl_3$) = 26.302948).[33] Peaks are reported either as singlets (s), doublets (d), triplets (t), or as combinations thereof, unless the signals are severely broadened (b), overlapped, or otherwise unresolvable, in which case they are represented as multiplets (m). The coupling constants J are given in Hz. High-resolution mass spectra were recorded on a Bruker Daltonics MicroTOF-Q II electrospray ionization time-of-flight (ESI-TOF) mass spectrometer in the negative polarization mode using 5 mM sodium formate solution for calibration. MS results are given as anionic mass peaks as m/z (mass to charge) ratio. Gas chromatography was performed with both flame ionization and mass detectors (FID and MS, respectively). GC-FID is equipped with HP-1 column (30m × 320 μm × 0.25 μm), and He as the carrier gas, using the following temperature program: Inlet 250 °C, oven $T_{initial}$ = 80 °C (8 min), rate 10 °C/min, T_{final} = 300 °C, hold 5 min. GC-MS is

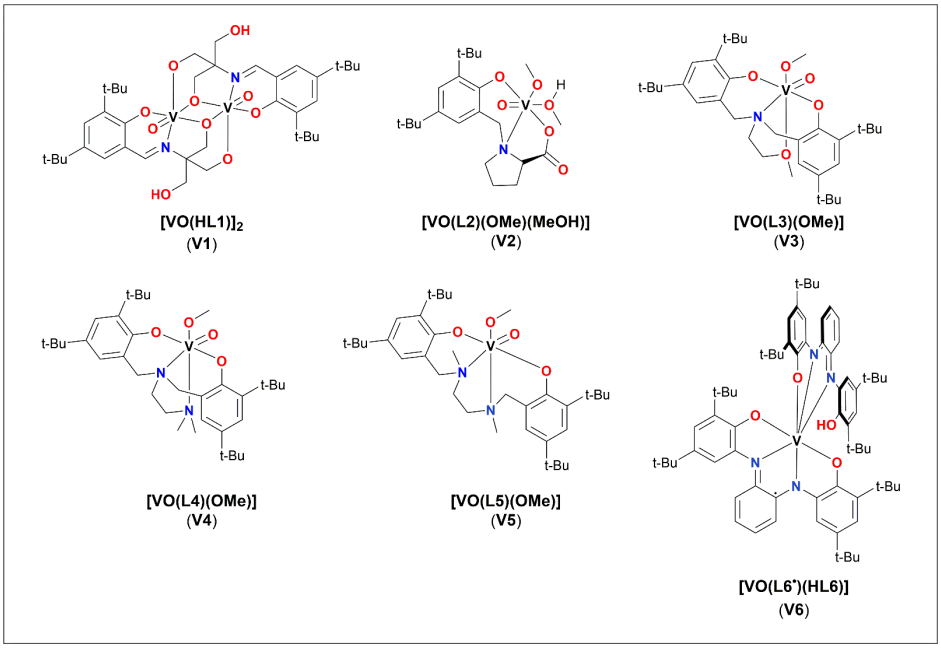

Figure 1. The structures of the vanadium complexes supported by multidentate aminophenolate-type ligands used in this study. Additionally, see the structures of the free ligands in the ESI Scheme S1.

equipped with Triple-Axis Detector, HP-5MS column (30m × 250 µm × 0.25 µm), and He as the carrier gas, using the following temperature program: Inlet 250 °C, oven $T_{initial}$ = 80 °C (4 min), rate 25 °C/min, T_{final} = 300 °C, hold 10 min. All EPR spectra were recorded under ambient atmospheric conditions at RT on a Freiberg Instruments Miniscope X-band EPR spectrophotometer using a *ca.* 1–2 mM vanadium sample concentration. The full scan EPR spectra were recorded from 25 to 650 mT (250 to 6500 G), and center field scans were performed from 334 to 339.5 mT (3340 to 3395 G) with a sweep time of 60 s, 0.100 mT signal modulation and 100 % microwave power, power, with a 0 dB attenuation.

Syntheses

The syntheses of all compounds were performed according to known literature procedures or with slight modifications. The structures of the proligands are additionally shown in the ESI figure S1.

H_4L1[24,26] In a 100 mL round-bottomed flask equipped with a magnetic stir-bar and a reflux condenser was placed 2.34 g (10 mmol) 3,5-di-*tert*-butylsalicylaldehyde and 1.21 g (10 mmol) tris(hydroxymethyl)aminomethane (10 mmol). All solids were dissolved in 20 mL absolute ethanol and the resulting reaction mixture was refluxed for *ca.* four hours, cooled, and rotaevaporated to dryness to yield a yellow solid. The solid was washed with small amounts of ice-cold dichloromethane to furnish the target compound as a brightly yellow powder. ^{1}H NMR (DMSO-d6,298 K, 600 MHz, TMS) δ 14.90 (1H, d, J = 2.2 Hz), 8.55 (1H, d, J = 2.2 Hz), 7.27 (1H, d, J = 2.5 Hz), 7.22 (1H, d, J = 2.5 Hz,), 4.70 (3H, t, J = 5.4 Hz), 3.62 (6H, d, J = 5.4 Hz), 1.37 (9H, s), 1.27 (9H, s). ^{13}C NMR (DMSO-d6, 151 MHz, 298 K, TMS) δ 165.4, 160.2, 138.1, 136.2, 126.8, 126.0, 117.5, 66.8, 61.4, 34.6, 33.8, 31.3, 29.3.

[VO(H_2L1)]$_2$ (V1)[24] To a 100 mL Erlenmeyer flask equipped with a magnetic stir-bar was weighed 337 mg (1.0 mmol) **H_4L1** and 265 mg (1.0 mmol) [VO(acac)2]. The solids were dissolved in ca. 15 mL methanol and upon ca. 15 minutes of stirring at RT, an umber-colored solid precipitated out of solution. The solid was collected by filtration, washed with RT methanol, and air-dried to afford the target compound in a pure non-crystalline form. Re-crystallization from hot acetonitrile yielded dark crystals of the pure compound. ^{1}H NMR (acetone-d6, 600 MHz, 298 K, TMS) δ 9.08 (1H, s), 7.66 (1H, d, J = 2.5 Hz), 7.53 (1H, d, J = 2.5 Hz), 5.25(1H, d, J = 14.3 Hz), 5.13 (2H, m), 4.70 (1H, d, J = 8.9 Hz), 4.58 (1H, t, J = 5.4 Hz), 4.04 (2H, dd, J1 = 5.6 Hz, J2 = 3.2), 1.51(9H, s), 1.35 (9H, s). ^{13}C NMR (acetone-d6, 151 MHz, 298 K, TMS) δ 165.5, 161.0, 141.3, 137.8, 131.3, 129.7, 121.4, 85.9, 81.9, 79.7, 64.5, 36.0, 34.8, 31.7, 30.5. ^{51}V NMR (acetone-d6, 298 K, 132 MHz, $VOCl_3$) δ –562.

H_2L2[23] In a 100 mL round-bottomed flask equipped with a magnetic stir-bar and a reflux condenser was placed 4.13 g (20 mmol) 2,4-di-*tert*-butylphenol, 0.60 g (20 mmol) paraformaldehyde and 2.30 g (20 mmol) L-proline. All solids were dissolved in 30 mL methanol, and the resulting reaction mixture was stirred, heated to boil, and refluxed for *ca.* 16 h. The target compound was obtained *via* column chromatography (dichloromethane:methanol, gradient 100:0 to 9:1, V:V as eluent) as a light purple solid. ^{1}H NMR (CDCl3, 298 K, 400 MHz, TMS) δ 9.01 (s, 2H), 7.31 (d, 1H, J=2.2 Hz), 6.92 (d, 1H, J=2.2 Hz), 4.62 (d, 1H, J=13 Hz), 3.90 (d, 1H, J=13 Hz), 3.79 (t, 1H, J=7.0 Hz), 3.41 (m, 1H), 2.79 (q, 1H, J = 10 Hz), 2.30 (m, 2H), 1.95 (m, 2H), 1.41 (s, 9H), 1.27 (s, 9H). ^{13}C NMR (CDCl3, 298 K, 100 MHz, TMS) δ 173.7, 153.4, 141.9, 138.1, 125.3, 124.8, 120.1, 67.6, 56.8, 53.1, 35.0, 34.2, 31.6, 29.9, 28.7, 23.0.

[VO(L2)(OMe)(MeOH)] (V2)[23] In a 50 mL round-bottomed flask equipped with a magnetic stir-bar and a reflux condenser was weighed 333 mg (1.0 mmol) **H_2L2** and 265 mg (1.0 mmol)

$[VO(acac)_2]$. All solids were suspended in ca. 25 mL analytical grade methanol, and the resulting dark brown reaction mixture was heated to boil and refluxed for three hours. Afterwards, heating was stopped, the reaction mixture was cooled and transferred to a –25 °C freezer, whereupon dark brown crystals formed in several days. The crystals were isolated by vacuum filtration, washed with small amounts of ice-cold methanol, and air-dried to afford the target compound. **V2** displays several ^{51}V NMR signals due to conformers; the oxo, methoxo and methanol ligand may switch coordination sites. This behavior is very common in structurally similar oxovanadium complexes.[19,34,35] ^1H NMR (MeOH-d4, 298 K, 500 MHz, TMS) δ 7.44 (d, 1H, J = 2.3 Hz), 7.17 (d, 1H, J = 2.3 Hz), 4,05 (dd, 1H, J1 = 8.5 Hz, J2= 2.3 Hz), 3.81 (d, 1H, J = 12 Hz), 3.53 (d, 1H, J = 12.0 Hz), 3.37 (m, 1H), 3.21 (m, 1H), 2.39 (m, 2H), 2.06 (m, 1H), 1.89 (m, 1H), 1.50 (s, 9H), 1.34 (s, 9H). ^{51}V NMR (MeOH-d4, 298 K, 132 MHz, $VOCl_3$) δ −554, −493, −466.

H_2L3[36] In a 100 mL round-bottomed flask equipped with a magnetic stir-bar and a reflux condenser was weighed 4.13 g (20 mmol) 2,4-di-*tert*-butylphenol, 0.80 g (11 mmol) 2-methoxyethylamine and 3.10 mL (42 mmol) 37 w-% formaline. The neat reaction mixture was heated in an oil-bath at 125 °C for *ca.* 18 hours. After cooling, the resulting residue was taken up in minimal amount of methanol and stirred at RT until the target compound precipitated as a white solid. The white solid was isolated by vacuum filtration and washed with ice-cold methanol. ^1H NMR ($CDCl_3$, 500 MHz, 298 K, TMS): δ 8.48 (bs, 2H), 7.22 (d, J = 2.5 Hz, 2H), 6.89 (d, J = 2.5 Hz, 2H), 3.75 (s, 4H), 3.56 (t, J = 5.2 Hz, 2H), 3.47 (s, 3H), 2.75 (t, J = 5.2 Hz, 2H), 1.42 (s, 18H), 1.28 (s, 18H). ^{13}C NMR ($CDCl_3$, 125 MHz, 298 K, TMS): δ 153.0, 140.9, 136.2, 125.0, 123.6, 121.8, 71.6, 59.0, 58.2, 51.5, 35.1, 34.3, 31.8, 29.7.

[VO(L3)(OMe)] (**V3**)[25] In a 50 mL round-bottomed flask equipped with a magnetic stir-bar and a reflux condenser was weighed 512 mg (1.0 mmol) **H_2L3** and 253 mg (1.0 mmol) $VOSO_4 \cdot 5\ H_2O$. All solids were dissolved in 10 mL methanol, treated with 291 µL (2.1 mmol) triethylamine, and the resulting reaction mixture was heated to boil and refluxed for three hours. Subsequently, the reaction mixture cooled at RT, and stored in a –25 °C freezer for several days. The target compound was isolated by vacuum filtration as dark crystals, washed with ice-cold methanol and air-dried. ^1H NMR ($CDCl_3$, 500 MHz, 298 K, TMS): δ 7.30 (d, 2H), 6.97 (d, 2H), 5.27 (s, 3H), 4.56 (d, 2H), 3.82 (d), 3.37 (s, 3H), 3.24 (t, 2H), 2.84 (t, 2H), 1.47 (s, 18H), 1.30 (s, 18H). ^{51}V NMR ($CDCl_3$, 132 MHz, 298 K, $VOCl_3$): δ –499, –481, –458, –448.

H_2L4[36] In a 250 mL round-bottomed flask equipped with a magnetic stir-bar and a reflux condenser was weighed 8.26 g (40 mmol) 2,4-di-*tert*-butylphenol, 1.86 mL (20 mmol) *N*,*N*-dimethylethylenediamine and 3.00 mL (40 mmol) 37 w-% formaline. All reagents were suspended in 50 distilled water and refluxed for *ca.* 18 hours to obtain a brown solid. All solvents were subsequently decanted off, and the brown solid was taken up in 100 mL technical methanol. Upon stirring at RT, the target compound precipitated as a white solid and was isolated by vacuum filtration and washed with ice-cold methanol. ^1H NMR ($CDCl_3$, 500 MHz, 298 K, TMS): δ = 9.78 (s, 2H), 7.19 (d, J = 2.4 Hz, 2H), 6.87 (d, J = 2.4 Hz, 2H), 3.60 (s, 4H), 2.58 (m, 4H), 2.30 (s, 6H), 1.38 (s, 18H), 1.26 (s, 18H).

[VO(L4)(OMe)] (**V4**)[37] In a 50 mL round-bottomed flask equipped with a magnetic stir-bar and a reflux condenser was weighed 525 mg (1.0 mmol) **H_2L4** and 265 mg (1.0 mmol) $[VO(acac)_2]$. All solids were dissolved in *ca.* 20 mL analytical grade methanol, and the resulting dark blue reaction mixture was heated to boil and refluxed for three hours. Afterwards, heating was stopped, the reaction mixture was cooled at RT and transferred to a –25 °C freezer and stored there overnight, whereupon dark red crystals formed. The crystals were isolated by vacuum filtration, washed with small amounts of ice-cold methanol, and air-dried to afford the target compound. ^1H NMR ($CDCl_3$, 500 MHz, 298 K, TMS): δ 7.29 (s, 2H), 7.00 (s, 2H), 5.20 (s, 4H), 2.57 (s, 6H), 1.57 (s, 3H), 1.55 (t, 4H), 1.50 (s, 18H), 1.28 (s, 18H). ^{51}V NMR ($CDCl_3$, 132 MHz, 298 K, $VOCl_3$): δ –460, –439, –371, –348.

H_2L5[36] In a 100 mL round-bottomed flask equipped with a magnetic stir-bar and a reflux condenser was weighed 8.26 g (40 mmol) 2,4-di-*tert*-butylphenol, 1.76 g (20 mmol) *N*,*N'*-dimethylethylenediamine and 3.00 mL (40 mmol) 37 w-% formaline. All reagents were dissolved in 50 mL methanol and refluxed for *ca.* 18 hours. Subsequently, the reaction mixture was stored in a –25 °C whereupon the target compound precipitated as a white solid. The solid was isolated by vacuum filtration and washed with ice-cold methanol.

[VO(L5)(OMe)] (**V5**)[38] In a 50 mL round-bottomed flask equipped with a magnetic stir-bar and a reflux condenser was weighed 525 mg (1.0 mmol) **H_2L5** and 253 mg (1.0 mmol) $VOSO_4 \cdot 5\ H_2O$. All solids were dissolved in 10 mL methanol, treated with 291 µL (2.1 mmol) triethylamine, and the resulting reaction mixture was heated to boil and refluxed for three hours. Subsequently, the reaction mixture was allowed to cool at RT, stored in a –25 °C freezer for several days. The target compound was isolated by vacuum filtration as dark crystals, which were washed with ice-cold methanol and air-dried. ^1H NMR (toluene-d8, 500 MHz, 298 K, TMS): δ 7.51 (d, J = 2.9 Hz, 2H), 7.51 (dd, J1 = 2.5 Hz, J2 = 6.7 Hz, 2H), 4.52 (d, J = 14.5 Hz, 1H), 4.40 (d, J = 13.6 Hz, 1H), 3.12 (d, J = 14.5 Hz, 1H), 2.83 (d, J = 13.6 Hz, 1H), 2.63 (d, J = 10.0 Hz, 2H), 2.24 (s, 3H), 2.13 (s, 3H), 1.77 (s, 9H), 1.66 (s, 9H), 1.39 (s, 9H), 1.35 (s, 9H). ^{51}V NMR (toluene-d8, 132 MHz, 298 K, $VOCl_3$): δ –473.

H_4L6[39] In a 100 mL round-bottomed flask quipped with a magnetic stir-bar was weighed 4.00 g (18 mmol) 3,5-di-*tert*-butylcatechol and 1.00 g (9 mmol) 1,2-diamino-benzene. All solids were dissolved in *n*-hexane, treated with a catalytic amount of triethylamine (~1 drop), resulting in a darkasdsadassdadasdsadsadsadsadsadsadsadasdsadasdsadasd asdasdsadsadas reaction mixture. The reaction mixture was stirred at RT in an open flask for two days, after which it was vacuum filtered to afford a white solid. The solid was washed with small amounts of ice-cold n-hexane to afford the target compound. 1H NMR ($CDCl_3$, 500 MHz, 298 K, TMS): δ 7.15 (d, J = 2.3 Hz, 2H), 6.89 (d, J = 2.3 Hz, 2H), 6.88 (dd, J1 = 5.8 Hz, J2 =

Table 1. Stoichiometry of vanadium pre-catalysts **V1**–**V6** and **1** used in the column chromatography experiments.

Pre-catalyst	Amount of pre-catalyst (mg/ µmol)	Amount of **1** (mg/ mmol)	[V]:[**1**]
V1	7.5/ 9.3	1000/ 4.5	1:481
V2	6.9/ 15	1001/ 4.5	1:300
V3	4.5/ 7.4	1000/ 4.5	1:608
V4	5.8/ 9	1000/ 4.5	1:500
V5	5.7/ 9.2	1000/ 4.5	1:490
V6	5.5/ 5.1	1000/ 4.5	1:881

Standard reaction conditions: Three-necked 250 mL round-bottomed flask equipped with a O_2 inlet, reflux condenser and magnetic stir bar. Reactions were maintained at 65 °C for 21–53 h, under 100 % O_2 pressure slightly above 1 atm in 60 mL 1,2-dichloromethane. See **table 5** for results.

Table 2. Stoichiometry of **1** and several additives in the control reactions.

Control reaction	Atm.	Amount of **1** (mg/ mmol)	Additive	Amount of additive rel. **1** (mol-% or eq.)
1	O_2	100/ 0.45	N/A	N/A
2	O_2	100/ 0.45	**H_2L4**	2.4 mg/ 4.5 µmol (1 mol-%)
3	O_2	202/ 0.91	Et_3N	1.25 µL/ 9.1 µmol (1 mol-%)
4	N_2	200/ 0.90	**V1**	7.20 mg/ 9.0 µmol **V1**(1 mol-%)
5	N_2	201/ 0.90	**V1** + H_2O_2 (2 eq.)	7.22 mg/ 9.0 µmol (1 mol-%) **V1** + 184 µL/ 1.80 mmol (2 eq.) H_2O_2
6	N_2	200/ 0.90	H_2O_2 (2 eq.)	184 µL/ 1.80 mmol (2 eq.)

Standard reaction conditions: Two-necked 100 mL round-bottomed flask equipped with a gas inlet, reflux condenser and magnetic stir bar. Reactions were maintained at 65 °C for *ca.* 48 h, under 100 % O_2 or N_2 pressure slightly above 1 atm in 6–25 mL 1,2-dichloromethane. See **table 5** for results.

3.5 Hz), 6.67 (dd, J1 = 5.8 Hz, J2 = 3.5 Hz), 5.87 (s, 2H), 5.13 (s, 2H), 1.44 (s, 18H), 1.27 (s, 18H).

[V(L6•)(HL6)] (**V6**)[40] In a 50 mL round-bottomed flask equipped with a magnetic stir-bar was weighed 150 mg (0.29 mmol) **H_4L6** and 79 mg (0.31 mmol) $VOSO_4 \cdot 5\ H_2O$. All solids were dissolved in ca. 8 mL methanol, treated with 50 µL (0.36 mmol) triethylamine, affording a dark purple reaction mixture. The reaction was stirred at RT over a period of three days. The target compound is obtained from the methanol reaction mixture as black crystals after vacuum filtration. IR-ATR (cm^{-1}): 2951 (s), 2904 (s), 2867 (s), 1582 (w), 1446 (s), 1415 (m), 1391 (m), 1360 (s), 1334 (m), 1249 (vs), 1196 (s), 1160 (s), 1136 (s), 1112 (s), 1025 (m), 989 (m), 911 (m), 862 (w), 821 (w), 770 (w), 740 (s), 665 (m), 647 (m), 602 (w), 586 (w), 545 (m), 506 (m), 463 (m).

Catalysis

Product distribution – gas and column chromatography, ^{1}H NMR

The column chromatography product distribution experiments, *i.e.* the primary catalytic reactions involving **V1**–**V6** were performed following the Finke protocol, with very slight modifications.[28] For this purpose, several mg of **V1**–**V6** (< 1 mol-%) were mixed with ca. 1,000 mg **1** according to **Table 1** in a 250 mL three-necked round-bottomed flask equipped with a magnetic stir-bar, O_2 gas inlet, reflux condenser with balloon, and a stopper (reaction apparatus shown in ESI Figure S2). All solids were dissolved in 60 mL 1,2-dichloroethane saturated with O_2. The reactions were maintained at 65 °C for 21–52 hours (aluminum block heating) under slight overpressure O_2 atmosphere. The completion of the reactions was monitored using TLC (dichloromethane), and upon completion, the reactions were rotaevaporated to dryness. All products were isolated by column chromatography on silica gel using dichloromethane as the eluent (see ESI Figure S3). The fractions were analyzed by ^{1}H and ^{13}C NMR, and quantities estimated based on integrated peak areas (for mixtures). Products were identified according to published data.[28] A silica gel column sized ca. 3 cm x 45 cm (diameter x height) using ca. 250 mL Merck silica gel 60 (0.040–0.063 mm) was used for column chromatography. In the GC-FID/GC-MS product distribution experiments, 1–2 mg **V1**–**V6** were mixed with 150 mg **1** in 15 mL scintillation vials and dissolved in *ca.* 5 mL 1,2-

Table 3. Stoichiometry of pre-catalysts **V1**–**V6** and **1** used in the EPR experiments.

Pre-catalyst	Amount of pre-catalyst (mg/ µmol)	concentration of pre-catalyst (mM)	Amount of **1** (mg/ mmol)	[V]:[**1**]
V1	1.00/ 1.25	1.25	28/ 0.126	1:101
V2	1.00/ 2.33	2.33	44.5/ 0.200	1:100
V3	1.20/ 1.97	1.97	44.2/ 0.199	1:102
V4	1.25/ 2.01	2.01	44.5/ 0.200	1:100
V5	1.25/ 2.01	2.01	44.4/ 0.200	1:100
V6	2.15/ 2.00	2.00	44.6/ 0.201	1:101

Standard reaction conditions: The reagents were dissolved in 1.000 mL toluene in 8 mL vials with stirring, and subsequently injected into capillary tubes for EPR analysis.

Table 4. Stoichiometry of pre-catalysts and **1** used in the ^{51}V NMR and ESI-MS experiments.

Pre-catalyst	Amount of pre-catalyst (mg/ µmol)	Amount of **1** (mg/ mmol)	[V]:[**1**]
V1	2.6/ 3.24	72/ 0.32	1:100
V2	5.1/ 11.9	264/ 1.19	1:100
V3	2.7/ 4.44	99/ 0.44	1:100
V4	2.5/ 4.03	91/ 0.40	1:100
V5	2.6/ 4.19	93/ 0.42	1:100
V6	4.0/ 3.71	83/ 0.37	1:100

Standard reaction conditions: The reagents were dissolved in 0.650 mL $CDCl_3$ in 8 mL vials with stirring, and subsequently filtered through a Celite plug in 5 mm o.d. NMR tubes. After ^{51}V NMR measurements, the samples were diluted to GC-MS ready acetonitrile for mass analysis.

dichloroethane. The reactions were maintained for ca. six days at RT under ambient atmosphere before gas chromatography analysis.

Product distribution – control reactions

A series of control experiments were performed to better understand the role of O_2 and H_2O_2, as well as the impact of several additives such as catalytic amounts of **V1**, triethylamine (Et_3N) or proligand **H_2L4** on the oxidation of **1** (**Table 2**). These reactions were performed in 1,2-dichloroethane under a steady stream of O_2 or N_2 using a similar apparatus as described in the ESI Figure S2.

Reaction monitoring – EPR

The negative mode ESI-MS experiments the EPR experiments were done with a [V]:[**1**] stoichiometry of *ca.* 1:100 according to **Table 3** to reflect the the column chromatography experiments. Additionally, samples were prepared in 1.000 mL toluene so that the concentration per vanadium center is *ca.* 2 mM. The samples were analyzed by EPR at reaction time *t* = 30 min, 6 h, 24 h, 48 h and 72 h. All EPR measurements were performed at RT under ambient conditions.

Reaction monitoring – ^{51}V NMR and negative mode ESI-MS

For ^{51}V NMR, solutions containing *ca.* 1:100 (pre-catalyst: **1**) were prepared in 650 µL $CDCl_3$ according to **Table 4** to reflect the stoichiometry used in the column chromatography experiments. After ^{51}V NMR measurements, the NMR samples were diluted in hyper grade GC-MS ready acetonitrile for mass analysis. Initial "during reaction" ^{51}V NMR and ESI-MS measurements are done immediately after dissolution of **V1**–**V6** and **1**, whereas "post-reaction" measurements are done after 48 hours of reaction onset.

Results and discussion

Product distribution

The aerobic oxidation of **1** in the presence of catalytic amounts of **V1**–**V5** as well as the previously unevaluated **V6** affords, in each case, a characteristic[27,29,30] product distribution, with little variation between the pre-catalysts, as determined by gas chromatography (**Figure 2** and ESI). Specifically, the catalytic oxidation of **1** by **V1**–**V6** affords the autoxidation product **2**, 3,5-di-*tert*-butyl muconic acid anhydride (**3**), lactones 4,6-di-*tert*-butyl-2-pyrone (**4a**) and 3,5-di-*tert*-butyl-2-pyrone

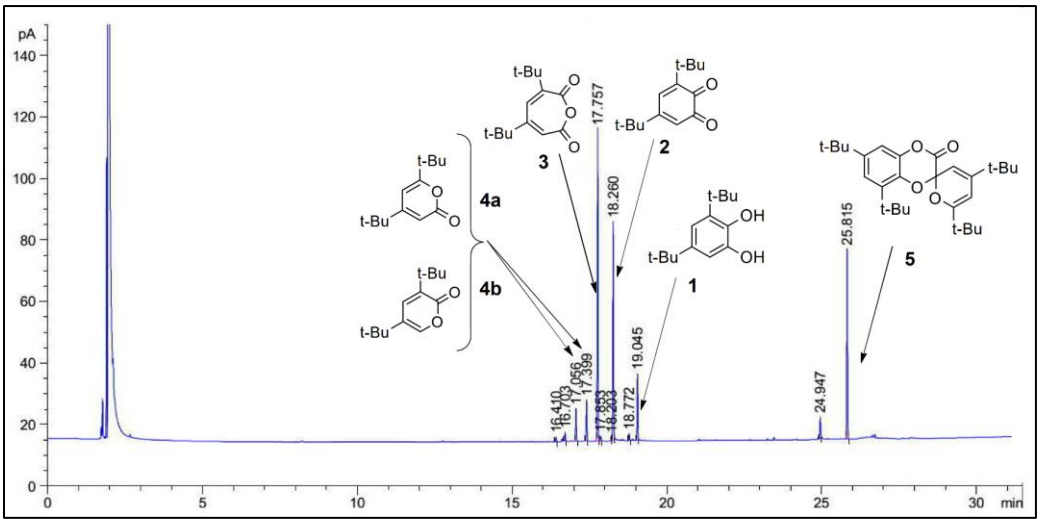

Figure 2. Gas chromatogram showing the product distribution as obtained for **V1**-catalyzed aerobic oxidation of **1**. A very similar product distribution is obtained with **V2**–**V6** (ESI figures S11–S15).

(**4b**), as well as the spiro-product, 4',6,6',8-tetra-*tert*-butyl-*3H*-spiro[benzo-[b][1,4]-dioxine-2,2'-pyran]-3-one (**5**). An acid product 3,5-di-*tert*-butyl-5-(carboxymethyl)-2-furanone (**6**), which has been reported to be among the oxidation products[27,29,30] is, however, not detected. It is nonetheless noteworthy that the product **4b** has not been, to the best of our knowledge, observed before in V-catalyzed oxidation of **1**.[27,29,30]

Attempts were made to quantify the yields of **2**–**5** by means of column chromatography (**Table 5**). The products **2** and **3**, which are easily visible in the column, are easily and reliably isolated in all cases with yields of 16–21 % and 30–39 %, respectively, corresponding to approx. half of the total mass balance. The yields for **2** and **3** obtained in this study well reflect that obtained by Finke and co-workers: The yield for **2** is well within the reported limits (16-21 % *vs.* 9-25 %). The isolated yield for **3** is somewhat less than reported (30-39 % *vs.* 40-57 %). However, for **2** and **3** the general trend is similar than what Finke and co-workers have reported, namely that **3** is clearly obtained as the main product, with **2** being second to that. Products **4a** and **4b**, as well as **5** are minor products, and they could be isolated with varying success. The isolated yields of **4** (0-26 % *vs.* 6-15 %) and **5** (0-7 % *vs.* 10-18 %) display the highest discrepancy from the reported. However, it is interesting to note that we were able to isolate **4b**, the structural isomer of **4a**, which to the best of our knowledge has not been previously reported to be among the V-catalyzed **1** oxidation products.[27,29,30] **4b** was also isolated when **V1**–**V3** was used as the pre-catalysts (**table 5** entries 2–4). We were unable to detect (GC), nor isolate, **6** by column chromatography. Generally, the product distribution involving the main products **2** and **3** is similar to the reports of Finke and co-workers. While the remaining products **4** and **5** represent minor products only, and their successful isolation was only partial, the product distribution experiments regardless show that **2** is not the only product, nor even the most abundant, as previously surmised.

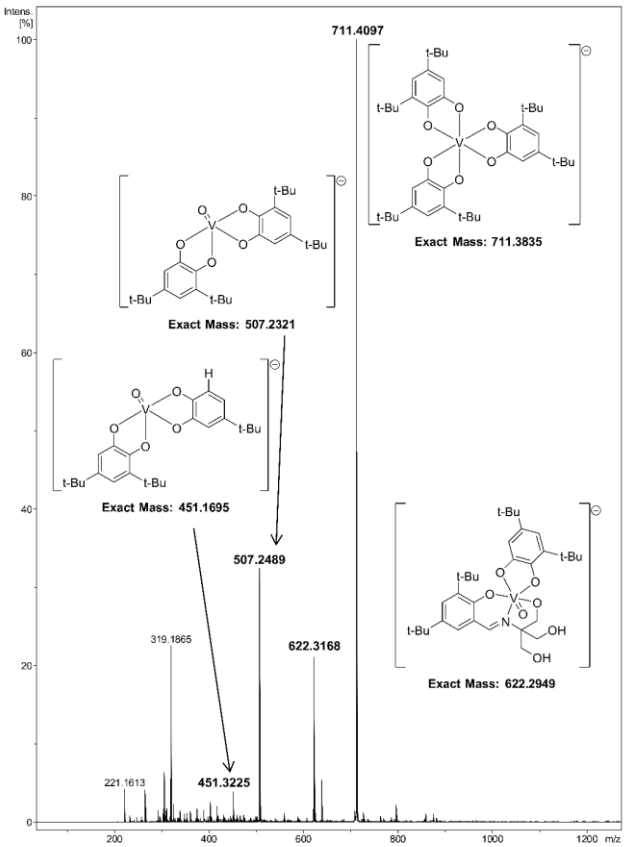

Figure 3. Negative mode ESI-MS spectrum showing the speciation between m/z = 0 – 1250 after treatment of **V1** with 100 eq. **1**. A very similar ESI-MS speciation is obtained for **V2**–**V6** (ESI figures S20–S29)

ARTICLE

Table 5. The characteristic product distribution obtained in the catalytic aerobic oxidation of **1** by **V1**–**V6** using a modified Finke protocol. The products were isolated by column chromatography. Conversion estimated by TLC or ^{1}H NMR.

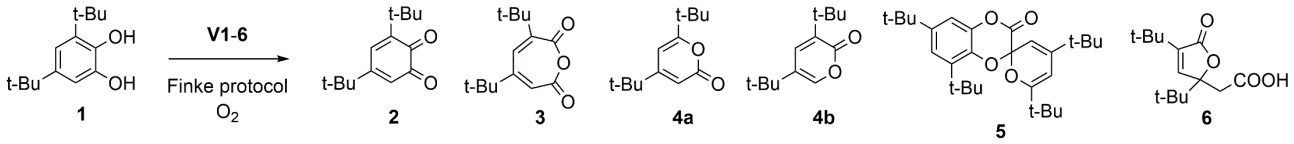

		Product distribution									
Entry	Pre-catalyst	**2**	**3**	**4a**	**4b**	**5**	**6**	Conv. (%)	Total isolated yield (%)	Refs.	Time (h)
1	**Previous studies**	9–25	40–57	6–15	N/A	10–18	<5	≥ 95		[27,29,30]	~300
2	**V1**	16	30	17	9	4	0	≥ 95	76	[a]	21
3	**V2**	21	35	4	5	0	0	≥ 95	65	[a]	52
4	**V3**	19	33	17	5	5	0	≥ 95	79	[a]	21
5	**V4**	16	39	0	0	7	0	≥ 95	62	[a]	44
6	**V5**	19	38	0	0	0	0	≥ 95	57	[a]	53
7	**V6**	18	38	0	0	0	0	≥ 95	56	[a]	44
8	**control 1**	5	0	0	0	0	0	5	5[b]	[a]	48
9	**control 2**	7	0	0	0	0	0	7	7[b]	[a]	48
10	**control 3**	24	1	0	0	0	0	25	25[b]	[a]	48
11	**control 4**	0	0	0	0	0	0	0	0[b]	[a]	48
12	**control 5**	94	6	0	0	0	0	100	100[b]	[a]	48.5
13	**control 6**	44	1	0	0	0	0	55	55[b]	[a]	48

Finke protocol reaction conditions: 1.000 g **1**, 5–9 mg (1 mol-%) **V1–V6** in 60 mL 1,2-dichloroethane under 100 % O_2, *t* = 21–53 h, *T* = 65 °C. See Table 2 and ESI for further details. [a] This work. [b] Non-isolated yield determined using ^{1}H NMR. Control reactions were performed in 25 mL Schlenk-bottles or 100 mL 2-necked round-bottomed flasks equipped with magnetic stir-bars under 100 % O_2/N_2 atmosphere at *T* = 65 °C with the following conditions: **Control 1**: 100 mg **1** (0.45 mmol), 6 mL 1,2-DCE, O_2. **Control 2**: 100 mg **1** (0.45 mmol), 2.4 mg **H_4L1** (4.57×10^{-3} mmol) 6 mL 1,2-DCE, O_2. 100 mg **1** (0.45 mmol), 6 mL 1,2-DCE, O_2. **Control 3**: 202 mg **1** (0.91 mmol), 1.25 µL Et_3N (9.0×10^{-3} mmol), 30 mL 1,2-DCE, O_2. **Control 4**: 200 mg **1** (0.90 mmol), 7.20 mg **V1** (9.0×10^{-3} mmol), 30 mL 1,2-DCE, N_2. **Control 5**: 201 mg **1** (0.90 mmol), 7.22 mg **V1** (9.0×10^{-3} mmol), 0.184 mL 30 w-% H_2O_2 (1.80 mmol), 30 mL 1,2-DCE, N_2. **Control 6**: 200 mg **1** (0.90 mmol), 0.184 mL 30 w-% H_2O_2 (1.80 mmol), 30 mL 1,2-DCE, N_2.

Control reactions – product distribution

Control reactions were performed with and without vanadium pre-catalysts and several additives in order to gain more insight regarding the product distribution in the oxidation of **1**. To verify whether **2** is obtained partly by autoxidation, the oxidation of **1** was performed in a 100 % O_2 atmosphere without **V1**–**V6** (control 1): The oxidation of **1** under 100 % O_2 without **V1**–**V6** affords solely **2** with an NMR yield of *ca.* 5 % in 48 hours, thus revealing the low but non-negligible, and autoxidative component of its oxidation (**Table 5**, entry 8).

The conversion from the O_2 driven autoxidation of **1** (*ca.* 5 %) is, however, significantly lower than what is observed in the presence of **V1**–**V6** (16–21 %). The autoxidation of **1** under aerobic, and especially alkaline conditions is well known.[41] Since **V1**–**V6** are partly converted in the presence of 100 eq. **1** to mixed catecholate bearing complexes (see below), it is expected that the ligands **L1**–**L6** must be partly released in solution. All proligands contain either imine or amine functionalities, making them basic to a certain extent. Thus, the oxidation of **1** was evaluated in the presence of 1 mol-% **H_2L4**, to verify whether the free ligands confer any base-catalytic properties themselves (control 2). The proligand **H_2L4** was specifically selected, as it contains two amine (basic) moieties, and 1 mol-% was chosen to reflect the situation assuming ligand **L4** was quantitatively released from **V4**. The effect of 1 mol-% **H_2L4** in the oxidation of **1** was found to be superficial, with an NMR conversion of 7 % obtained, a result within experimental error (**Table 5**, entry 9) when compared to entry 8.

Although the presence of 1 mol-% **H_2L4** barely affected the conversion of **1** in 48 hours, we were interested to learn if a catalytic amount added organic base such as triethylamine (Et_3N) would affect the oxidation of **1** (control 3) in any way, and in the absence of **V1**–**V6**. We deemed this control valid, since in some reports vanadium-catalyzed catechol oxidation is performed in the presence of stoichiometric amounts of base.[18]

It turns out that the oxidation of **1** was significantly affected by 1 mol-% Et_3N in the absence of **V1**–**V6**, affording **2** with a yield and a total conversion of *ca.* 24 % and 25 %, respectively (**table 5**, entry 10). Interestingly, and rather unexpectedly, the anhydride **3** was also obtained with a *ca.* 1 % yield (**Table 5**, entry 10). The modest formation of **3** in the latter reaction may be attributable to H_2O_2-driven Baeyer-Villiger-like (over)oxidation of **2** to **3**, which has been reported to occur *via* the stoichiometric oxidation by peracids.[42,43] A tentative H_2O_2-driven reaction mechanism has been proposed in ESI Scheme S2. In the proposed mechanism, the action of Lewis acids such as vanadium(v) may be reasonably expected to catalyze the reaction.

H_2O_2 participation in the formation of the common catalyst

While the dioxygenase products **3**–**5** require dioxygen (with the exception of **3**, which may be obtained from the overoxidation of **2** by peracids and H_2O_2, as described above), we were interested to learn whether H_2O_2 can oxidize **1** in the *absence* of O_2. Earlier we showed that **1** is indeed very slowly oxidized to **2** at RT in air and in the presence of three eq. H_2O_2.[24] The reaction rate could be increased in the presence of 1 mol-% **V1**.[24] Further control reactions were carried out under *anaerobic* conditions to learn more about the role of H_2O_2 in the oxidation of **1** (controls 4–6). As expected, no reaction occurs when **1** is maintained at 65 °C for 48 hours under N_2 atmosphere in the presence of 1 mol-% **V1** (**Table 5**, control 4, entry 11). In the control reaction 4, O_2 is not available to be converted to H_2O_2. However, once two eq. H_2O_2 is added relative to **1**, in the absence of O_2, full conversion is reached in the presence of 1 mol-% **V1**, with **2** and **3** being obtained in 94 % and 6 % yield, respectively (**Table 5**, control 5, entry 12). The control reaction 5 reveals that **1** may be substantially oxidized to **2** by H_2O_2 in the presence of **V1**. It also reveals that the catalytic dioxygenase pathways are not available, since O_2 is not present, explaining the lack of **4** and **5** in the products. The role of vanadium as catalyst in the reaction is highlighted since the yields of **2** and **3** are significantly lowered to 44 % and 1 %, respectively, in the absence of **V1** (**Table 5**, control 6, entry 13).

The anaerobic control reactions 4–6 (**Table 5** entries 11–13) hint that **1** is oxidized by H_2O_2 in addition to O_2, both catalytically and non-catalytically. In the initial step, **1** is oxidized by O_2 generating **2** and H_2O_2, the latter of which may further react with **1**, generating water. However, it should be emphasized that in the **V1**–**V6** catalyzed reactions (**Table 5** entries 2–7, with no added H_2O_2) the yield of the H_2O_2 produced from O_2 would be at most 16–21 % (*i.e.*, concomitant to the formation of **2**), somewhat limiting the actual impact of the H_2O_2-driven oxidation of **1**. Another interesting point is the anaerobic formation of **3** with or without **V1** as catalyst. A possible explanation is H_2O_2-mediated Lewis acid catalyzed (*e.g.*, V(v)) Baeyer-Villiger-like oxidation of **2** (ESI).[42,43]

EPR evidence of common catalyst

The aerobic oxidation of **1** in the presence of **V1**–**V6** was monitored by EPR spectroscopy for a period of 72 hours to gain insight into the overall catalytic mechanism. EPR spectra were recorded at reaction time *t* = 30 min, 6, 24, 48 and 72 hours in toluene at RT and in ambient conditions. Paramagnetic species are immediately formed upon treatment of **V1**–**V6** by 100 eq. **1**. The exact nature of the paramagnetic species is unknown in the case of **V1** and **V3**–**V6**. However, with **V2**, a 10-line spectrum, with a g factor ~ 2.0036 and a $A(^{51}V)$ ~ 2.05 G is observed. This spectrum is in good agreement with the structurally characterized $[V(3,5\text{-DTBC})_2(3,5\text{-DTBSQ}^{\bullet})]$ as reported by Pierpont and co-workers (see ESI figures S30a–f for the 30 min spectra).[11] Upon further slight progression of the reactions, at *t* = 6 h, the spectra have not undergone significant changes (ESI figures S31a–f).

EPR spectra recorded at *t* = 24 h after treatment of **V1**–**V6** with 100 eq. **1** begin to show significant changes when compared to the 30 min and 6 h spectra, respectively (ESI figures S32a–f). For example, **V1** shows an 11-line EPR spectrum (ESI figure S32a) with g factor ~ 2.0034 and $A(^{51}V)$ ~ 2.95 G, very close to the values reported for Pierpont's complex (g ~ 2.004–2.006, $A(^{51}V)$ = 3.05 G).[11] The 11-line spectrum may suggest that $[V(3,5\text{-DTBC})_2(3,5\text{-DTBSQ}^{\bullet})]$, which has a 10-line spectrum, might also be present in some proportion. Complexes **V3** and **V5**, on the other hand, both afford a 10-line EPR spectrum (ESI figure S32c and e) with g factors 2.0036 and 2.0037, and ^{51}V hyperfine coupling constants of 2.09 and 2.07 G, respectively. Both agree well with the 10-line EPR spectrum reported for $[V(3,5\text{-DTBC})_2(3,5\text{-DTBSQ}^{\bullet})]$ with a $A(^{51}V)$ = 2.1 G and g factor = 2.004.[11] In contrast, the EPR spectrum of **V6** is poorly resolved, but is beginning to show changes towards the formation of $[V(3,5\text{-DTBC})_2(3,5\text{-DTBSQ}^{\bullet})]$ (ESI figure S32f). **V2** affords the most interesting EPR spectrum, clearly showing at least two distinct EPR signals (ESI figure S32b). Namely, a 10-line spectrum having a g ~ 2.0035 and $A(^{51}V)$ = 2.05 G consistent with $[V(3,5\text{-DTBC})_2(3,5\text{-DTBSQ}^{\bullet})]$ is observed at the center field. Additionally, an eight-line EPR signal with g ~ 2.0021 and $A(^{51}V)$ = 8.91 G is visible in the background.

The EPR spectra recorded for **V1** and **V3**–**V6** at *t* = 48 h provide irrefutable evidence of the presence of Pierpont's complex (figure 4a and 4c–f). These EPR spectra, with an average ^{51}V hyperfine coupling constants of *ca.* 2.98 – 3.12 G and g factors approaching 2.0040, are characteristic to the Pierpont's complex.[11] As was observed at *t* = 24 h, and in the case of **V2** only, an intensive 8-line EPR spectrum with a $A(^{51}V)$ ~ 8.60 G and g factor ~ 2.0020 is obtained, in stark contrast to the other pre-catalysts (**Figure 4b**). According to ESI-MS, $[VO(L2)(3,5\text{-DTBSQ}^{\bullet})]$ is present as a major species in the reaction mixture at *t* = 48 h (ESI figure S34). We have thus tentatively assigned the eight-line EPR spectra to this species. Further details in the ESI. After 72 hours the EPR spectra of all reactions start to show considerable deterioration of the EPR signals. This is expected, since Pierpont's complex is known to be oxygen sensitive, slowly decomposing into V_2O_5 and free 3,5-DTBQ.[11,27] Thus, the 72-hour measurements signify the end of the EPR reaction monitoring experiments.

During the EPR measurements, it was observed that **V2** showed rather distinct behavior with respect to the other pre-catalysts. Specifically, it takes nearly 48 hours for the EPR

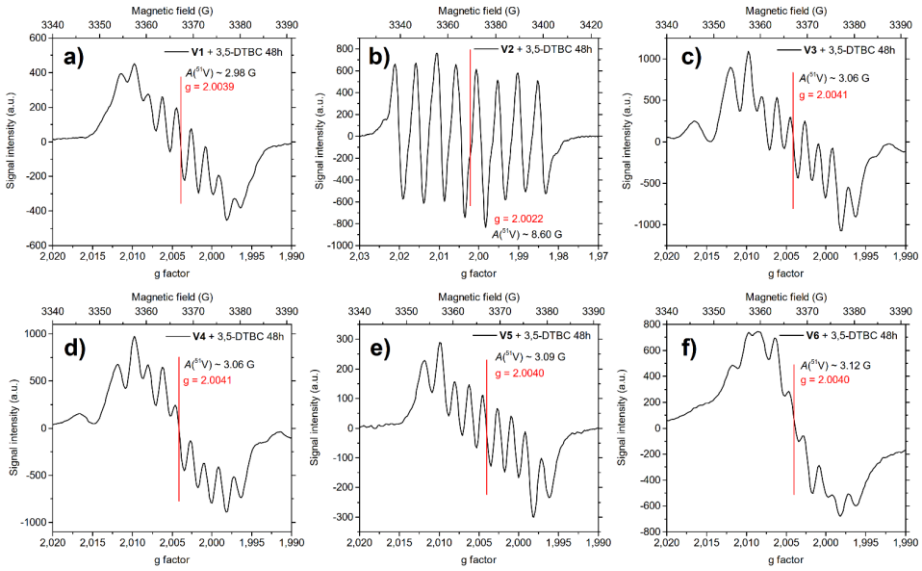

Figure 4. The ambient atmosphere center-field EPR spectra of reaction mixtures containing **V1**–**V6** and 100 eq. **1** in toluene recorded at RT 48 hours after reaction onset.

spectra corresponding to $[V(3,5\text{-DTBC})_2(3,5\text{-DTBSQ}^{\bullet})]$ or $[VO(3,5\text{-DTBC})_2(3,5\text{-DTBSQ}^{\bullet})]_2$ to be observed in the case of **V1** and **V3**–**V6**. In stark contrast, the 10-line spectra, corresponding to $[V(3,5\text{-DTBC})_2(3,5\text{-DTBSQ}^{\bullet})]$ is visible in the case of **V2** in 30 minutes already. Likewise, the formation of the tentative species $[VO(L2)(3,5\text{-DTBSQ}^{\bullet})]$, affording an eight-line spectrum with a $A(^{51}V)$ ~ 8.60 G and g ~ 2.0020, is distinctive for **V2** only. The different EPR behavior of **V2** may be explained in simple terms: **V2** is the only pre-catalyst supported by a *tridentate* ligand, which may be reasonably expected to offer less stabilization compared to the *tetradentate* ligands. Due to this, the consecutive conversion of **V2** into $[V(3,5\text{-DTBC})_2(3,5\text{-DTBSQ}^{\bullet})]$, $[VO(3,5\text{-DTBC})_2(3,5\text{-DTBSQ}^{\bullet})]_2$ as well as $[VO(L2)(3,5\text{-DTBSQ}^{\bullet})]$ is significantly more rapid when compared to **V1** and **V3**–**V6**. In other words, the lifetime of **V2** is much shorter than for the other complexes, manifesting as seemingly faster formation – and decomposition – of Pierpont's complex to $[VO(L2)(3,5\text{-DTBSQ}^{\bullet})]$.

^{51}V NMR and ESI-MS evidence of common catalyst

^{51}V NMR reveals that, in the case of **V1**–**V5** (**V6** being paramagnetic) upon treatment with 100 equivalents of **1** the original ^{51}V NMR signals corresponding to the vanadium catalyst precursors vanish entirely (ESI figure S16). These results suggest that a part of **V1**–**V5** is immediately converted to paramagnetic species, consistent with ESI-HRMS and EPR observations. For **V2**–**V5** the ^{51}V NMR spectra did not drastically change over the period of 48 hours (ESI figure S17). However, after 48 hours, and in the case of **V3**–**V4** a very faint ^{51}V NMR signal could be detected at approx. +1550 ppm, *significantly* downfield from the signals corresponding to the pre-catalysts themselves. Similarly to what we observed with **V1** in the earlier study,[24] we have tentatively assigned these ^{51}V NMR signals to catecholate bearing oxovanadium complexes, according to the studies by Rehder and Pecoraro.[15,44] By the same token, in the case of **V1**, a broad signal with a FWHM approaching 1 kHz at *ca*. –510 ppm has been tentatively assigned to $[VO(H_2L1)(3,5\text{-DTBC})]$, where H_2L1 is the doubly protonated iminophenolate ligand.[24] Further details in the ESI.

The above ^{51}V NMR samples were subsequently analyzed by negative mode ESI-MS during initial (t = 30 min) reaction and post-reaction at t = 48 hours. ESI-MS, as a semi-quantitative method is able to give reliable information about speciation in solution.[45,46] These measurements reveal that in each case **V1**–**V6** are nearly quantitatively converted to $[V(3,5\text{-DTBC})_3]^-$ and $[VO(3,5\text{-DTBC})_2]^-$ which have m/z = 711.3835 and m/z = 507.2321, respectively (**Figure 3**). Both are *diagnostic* species signaling the presence of the proposed active catalyst $[VO(3,5\text{-DTBC})(3,5\text{-DTBSQ}^{\bullet})]$[30] as well as its dimeric catalytic resting state, $[VO(3,5\text{-DTBC})(3,5\text{-DTBSQ}^{\bullet})]_2$.[27] However, the catalytic resting state, having a calculated m/z = 1014.4642, is not detected in any case. While there are no traces of intact **V1**–**V6** present, low-intensity species with a general formula $[VO(L)(3,5\text{-DTBC})]^-$ are detected with **V1**–**2**, **V4** and **V6** (ESI). The post-reaction mixtures after 48 hours show a rather similar ESI-MS speciation, with $[V(3,5\text{-DTBC})_3]^-$ remaining as the most intensive vanadium-containing species.

Conclusion

In summary and conclusion, the catechol oxidation mechanism of **V1**–**V6** was evaluated in the oxidation of **1** to critically re-assess earlier reports of **V1**–**V5** showing catechol oxidase mimetic activity, and to see if all complexes, including **V6**, obey the "common catalyst hypothesis" as proposed by Finke and co-workers. The GC and column chromatographic product distribution experiments reveal that all pre-catalysts not only *do not* display appreciable catechol oxidase activity, but rather *primarily* catechol dioxygenase activity. Specifically, a characteristic product distribution is obtained from the **V1**–**V6** catalyzed oxidation of **1**. From the oxidation products **2** is obtained by autoxidation, catalytic or otherwise, whereas **3**–**5** are catalytically produced intra- and extradiol dioxygenase

products. Moreover, extensive control reactions show that **1** may be oxidized to **2** with H_2O_2 as the terminal oxidant in lieu of O_2. Use of additives, particularly organic bases such as Et_3N moderately catalyze the oxidation of **1** to **2** at 1 mol-% loadings. Interestingly, **2** may be further oxidized to **3** by H_2O_2 in an anaerobic setting, not *via* a "dioxygenase" pathway, but rather a Baeyer-Villiger-like mechanism, as evidenced by detection of **3** in the absence of O_2.

EPR, ^{51}V NMR and ESI-MS experiments have provided convincing evidence to suggest that **V1**–**V6** indeed operate *via* the same mechanism as proposed by Finke and co-workers in the "common catalyst hypothesis". Namely, **V1**–**V6** leach vanadium by the action of H_2O_2, and are summarily converted in the presence of excess **1** to [VO(3,5-DTBC)(3,5-DTBSQ$^{\bullet}$)] – *i.e.* the common catalyst – which drives the formation of catechol dioxygenase products **3**–**5**. Even the complex **V6**, which is supported by two tetradentate ligands derived from **1**, was shown not to be exempt from the effects of vanadium leaching.

The results herein warrant further work to investigate if the other reported catechol oxidase mimicking vanadium pre-catalysts in fact display dioxygenase activity instead of the pursued oxidase activity. Furthermore, since it has been shown here that **V1**–**V6** readily leach vanadium in the presence of H_2O_2, further efforts should be made to mitigate this especially in the context of other oxidation catalysis, and particularly when structurally similar structurally similar complexes are used as pre-catalysts and H_2O_2 as the terminal oxidant.

Author Contributions

Pasi Salonen: Conceptualization, Investigation, Methodology, Visualization, Writing – original draft
Risto Savela: Investigation, Methodology, Visualization, Writing – review & editing
Anssi Peuronen: Visualization, Writing – review & editing
Ari Lehtonen: Supervision, Writing – review & editing

Conflicts of interest

There are no conflicts to declare.

Acknowledgements

Dr. Mika Keränen is greatly acknowledged for assistance in matters related to EPR spectroscopy. A.P. and P.S. gratefully acknowledge the Academy of Finland (project no. 315911), and University of Turku Graduate School (UTUGS) Doctoral Programme in Physical and Chemical Sciences (PCS) for funding, respectively.

References

1 R. A. Sheldon, I. W. C. E. Arends and U. Hanefeld, in *Green Chemistry and Catalysis*, Wiley, 2007, pp. 133–221.
2 C. L. Hill and I. A. Weinstock, *Nature*, 1997, **388**, 332–333.
3 R. H. Holm, P. Kennepohl and E. I. Solomon, *Chem. Rev.*, 1996, **96**, 2239–2314.
4 C. Gerdemann, C. Eicken and B. Krebs, *Acc. Chem. Res.*, 2002, **35**, 183–191.
5 J. B. Broderick, *Essays Biochem.*, 1999, **34**, 173–189.
6 A. L. Feig and S. J. Lippard, *Chem. Rev.*, 1994, **94**, 759–805.
7 M. NOZAKI, in *Molecular Mechanisms of Oxygen Activation*, Elsevier, 1974, vol. 1955, pp. 135–165.
8 S. K. Dey and A. Mukherjee, *Coord. Chem. Rev.*, 2016, **310**, 80–115.
9 I. A. Koval, P. Gamez, C. Belle, K. Selmeczi and J. Reedijk, *Chem. Soc. Rev.*, 2006, **35**, 814.
10 L. Que, R. C. Kolanczyk and L. S. White, *J. Am. Chem. Soc.*, 1987, **109**, 5373–5380.
11 M. E. Cass, D. L. Green, R. M. Buchanan and C. G. Pierpont, *J. Am. Chem. Soc.*, 1983, **105**, 2680–2686.
12 C. L. Simpson and C. G. Pierpont, *Inorg. Chem.*, 1992, **31**, 4308–4313.
13 S. R. Cooper, Y. B. Koh and K. N. Raymond, *J. Am. Chem. Soc.*, 1982, **104**, 5092–5102.
14 M. E. Cass, N. R. Gordon and C. G. Pierpont, *Inorg. Chem.*, 1986, **25**, 3962–3967.
15 C. R. Cornman, G. J. Colpas, J. D. Hoeschele, J. Kampf and V. L. Pecoraro, *J. Am. Chem. Soc.*, 1992, **114**, 9925–9933.
16 U. Casellato, S. Tamburini, P. A. Vigato, M. Vidali and D. E. Fenton, *Inorganica Chim. Acta*, 1984, **84**, 101–104.
17 Y. Tatsuno, M. Tatsuda and S. Otsuka, *J. Chem. Soc. Chem. Commun.*, 1982, **1982**, 1100.
18 A. A. El-Taras, I. M. EL-Mehasseb and A. E.-M. M. Ramadan, *Comptes Rendus Chim.*, 2012, **15**, 298–310.
19 M. R. Maurya, B. Uprety, F. Avecilla, P. Adão and J. Costa Pessoa, *Dalt. Trans.*, 2015, **44**, 17736–17755.
20 S. K. Mal, M. Mitra, H. R. Yadav, C. S. Purohit, A. R. Choudhury and R. Ghosh, *Polyhedron*, 2016, **111**, 118–122.
21 C. Balakrishnan and M. A. Neelakantan, *Inorganica Chim. Acta*, 2018, **469**, 503–514.
22 S. Ta, M. Ghosh, K. Ghosh, P. Brandão, V. Félix, S. K. Hira, P. P. Manna and D. Das, *ACS Appl. Bio Mater.*, 2019, **2**, 2802–2811.
23 P. Salonen, A. Peuronen, J. Sinkkonen and A. Lehtonen, *Inorganica Chim. Acta*, 2019, **489**, 108–114.
24 P. Salonen, A. Peuronen and A. Lehtonen, *Inorganica Chim. Acta*, 2020, **503**, 119414.
25 P. Salonen, A. Peuronen and A. Lehtonen, *Inorg. Chem. Commun.*, 2017, **86**, 165–167.
26 S. K. Dey and A. Mukherjee, *New J. Chem.*, 2014, **38**, 4985–4995.
27 C.-X. Yin and R. G. Finke, *J. Am. Chem. Soc.*, 2005, **127**, 9003–9013.
28 H. Weiner and R. G. Finke, *J. Am. Chem. Soc.*, 1999, **121**, 9831–9842.
29 C.-X. Yin, Y. Sasaki and R. G. Finke, *Inorg. Chem.*, 2005, **44**, 8521–8530.
30 C. X. Yin and R. G. Finke, *J. Am. Chem. Soc.*, 2005, **127**, 13988–13996.
31 A turnover frequency (k_{cat}) of 24.4 h^{-1} was obtained for **V2** in the aerobic oxidation of **1** in chloroform under ambient

conditions (unpublished results).
32 G. R. Fulmer, A. J. M. Miller, N. H. Sherden, H. E. Gottlieb, A. Nudelman, B. M. Stoltz, J. E. Bercaw and K. I. Goldberg, *Organometallics*, 2010, **29**, 2176–2179.
33 R. K. Harris, E. D. Becker, S. M. Cabral de Menezes, R. Goodfellow and P. Granger, *Magn. Reson. Chem.*, 2002, **40**, 489–505.
34 M. R. Maurya, B. Uprety, F. Avecilla, P. Adão, M. L. Kuznetsov and J. Costa Pessoa, *Eur. J. Inorg. Chem.*, 2017, **2017**, 3087–3099.
35 S. Barroso, P. Adão, F. Madeira, M. T. Duarte, J. C. Pessoa and A. M. Martins, *Inorg. Chem.*, 2010, **49**, 7452–7463.
36 E. Y. Tshuva, I. Goldberg, M. Kol and Z. Goldschmidt, *Organometallics*, 2001, **20**, 3017–3028.
37 D. Maity, A. Ray, W. S. Sheldrick, H. M. Figge, B. Bandyopadhyay and M. Ali, *Inorganica Chim. Acta*, 2006, **359**, 3197–3204.
38 M. Debnath, A. Dutta, S. Biswas, K. K. Das, H. M. Lee, J. Vícha, R. Marek, J. Marek and M. Ali, *Polyhedron*, 2013, **63**, 189–198.
39 P. Chaudhuri, M. Hess, J. Müller, K. Hildenbrand, E. Bill, T. Weyhermüller and K. Wieghardt, *J. Am. Chem. Soc.*, 1999, **121**, 9599–9610.
40 E. Salojärvi, A. Peuronen, M. Lahtinen, H. Huhtinen, L. S. Vlasenko, M. Lastusaari and A. Lehtonen, *Molecules*, 2020, **25**, 2531.
41 C. A. Tyson and A. E. Martell, *J. Phys. Chem.*, 1970, **74**, 2601–2610.
42 T. R. Demmin and M. M. Rogic, *J. Org. Chem.*, 1980, **45**, 1153–1156.
43 F. R. Hewgill and S. L. Lee, *J. Chem. Soc. C Org.*, 1969, 2080.
44 D. Rehder, C. Weidemann, A. Duch and W. Priebsch, *Inorg. Chem.*, 1988, **27**, 584–587.
45 M. J. Deery, T. Fernandez, O. W. Howarth and K. R. Jennings, *J. Chem. Soc. Dalt. Trans.*, 1998, 2177–2184.
46 S. Ralph, P. Iannitti, R. Kanitz and M. Sheil, *Eur. J. Mass Spectrom.*, 1996, **2**, 173.

